Symmetry-Breaking in Cationic Polymethine Dyes: Part 2. Shape of Electronic Absorption Bands Explained by the Thermal Fluctuations of the Solvent Reaction Field

ARTICLE *in* THE JOURNAL OF PHYSICAL CHEMISTRY A · JUNE 2015

Impact Factor: 2.69 · DOI: 10.1021/acs.jpca.5b03877 · Source: PubMed

THE JOURNAL OF PHYSICAL CHEMISTRY A

Article

pubs.acs.org/JPCA

Symmetry-Breaking in Cationic Polymethine Dyes: Part 2. Shape of Electronic Absorption Bands Explained by the Thermal Fluctuations of the Solvent Reaction Field

Artëm E. Masunov,*[,†,‡,§,∥] Dane Anderson,[†,‡] Alexandra Ya. Freidzon,[⊥,#] and Alexander A. Bagaturyants[⊥,#]

[†]NanoScienece Technology Center, [‡]Department of Chemistry, [§]Department of Physics, and [∥]Florida Solar Energy Center, University of Central Florida, 12424 Research Parkway, Ste 400, Orlando, Florida 32826, United States

[⊥]Photochemistry Center RAS, ul. Novatorov 7a, Moscow, 119421, Russia

[#]National Research Nuclear University MEPhI, Kashirskoye shosse 31, Moscow, 115409, Russia

ABSTRACT: The electronic absorption spectra of the symmetric cyanines exhibit dramatic dependence on the conjugated chain length: whereas short-chain homologues are characterized by the narrow and sharp absorption bands of high intensity, the long-chain homologues demonstrate very broad, structureless bands of low intensity. Spectra of the intermediate homologues combine both features. These broad bands are often explained using spontaneous symmetry-breaking and charge localization at one of the termini, and the combination of broad and sharp features was interpreted as coexistence of symmetric and asymmetric species in solution. These explanations were not supported by the first principle simulations until now. Here, we employ a combination of time-dependent density functional theory, a polarizable continuum model, and Franck−Condon (FC) approximation to predict the absorption line shapes for the series of 2-azaazulene and 1-methylpyridine-4-substituted polymethine dyes. To simulate inhomogeneous broadening by the solvent, the molecular structures are optimized in the presence of a finite electric field of various strengths. The calculated FC line shapes, averaged with the Boltzmann weights of different field strengths, reproduce the experimentally observed spectra closely. Although the polarizable continuum model accounts for the equilibrium solvent reaction field at absolute zero, the finite field accounts for the thermal fluctuations in the solvent, which break the symmetry of the solute molecule. This model of inhomogeneous broadening opens the possibility for computational studies of thermochromism. The choice of the global hybrid exchange-correlation functional SOGGA11-X, including 40% of the exact exchange, plays the critical role in the success of our model.

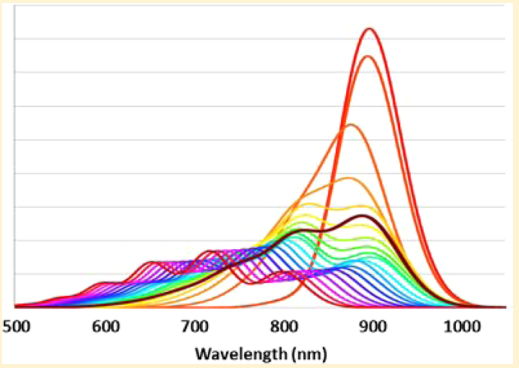

1. INTRODUCTION

Polymethine dyes, which contain an odd number of CH groups in their conjugated chains, are considered to be prospective candidates for the development of biophotonic and optoelectronic materials[1−7] because of their exceptional optical properties. In particular, they often possess high-intensity electronic absorption bands in the near-infrared (NIR) region. Substantial research efforts have been directed toward the rational design[8] of the new NIR polymethines that include various substituents and lengths of the conjugated chain.[9−12] Typically, when the polymethine chain length (C*n*) is increased by two CH groups, this results in a 100 nm red shift of the absorption maximum (so-called vinylene shift); however, when these rational design strategies were applied to di-2-azaazulene-terminated cationic polymethines (DAA*n* in Scheme 1),[13] the absorption intensity and peak sharpness were lost for the longer chain homologue DAA11 (Figure 1). The aim of this paper is to investigate the electronic mechanism of this loss.

The reasons for the described spectral changes were debated in the literature until a general consensus was reached in the paper by Tolbert and Zhao.[14] They argued that the shorter-chain cyanines are well described by equal contributions from two resonance structures (with the formal charge localized on the left and the right nitrogen atoms) as indicated by zero bond lengths alternation at the center of the chain. Meanwhile, in longer homologues, a spontaneous symmetry-breaking occurs, and one of the two resonance forms prevails. Thus, the charge localizes at one of the terminal groups, which results from a pseudo-Jahn−Teller effect also known as the Peierls distortion.[15] Tolbert and Zhao investigated a series DPY*n* polymethines (Scheme 1, Figure 2) and established that C13 (chain of 13 carbon atoms in DPY13) is sufficient to break symmetry in a polar solvent. The evidence for this symmetry breaking included the broad optical absorption band (similar to the intervalence electron transfer absorption in weakly coupled binuclear transition metal complexes[16]), stronger solvato-

Received: April 23, 2015
Revised: May 28, 2015

DOI: 10.1021/acs.jpca.5b03877
J. Phys. Chem. A XXXX, XXX, XXX−XXX

Scheme 1. Molecular Structures Investigated in This Work

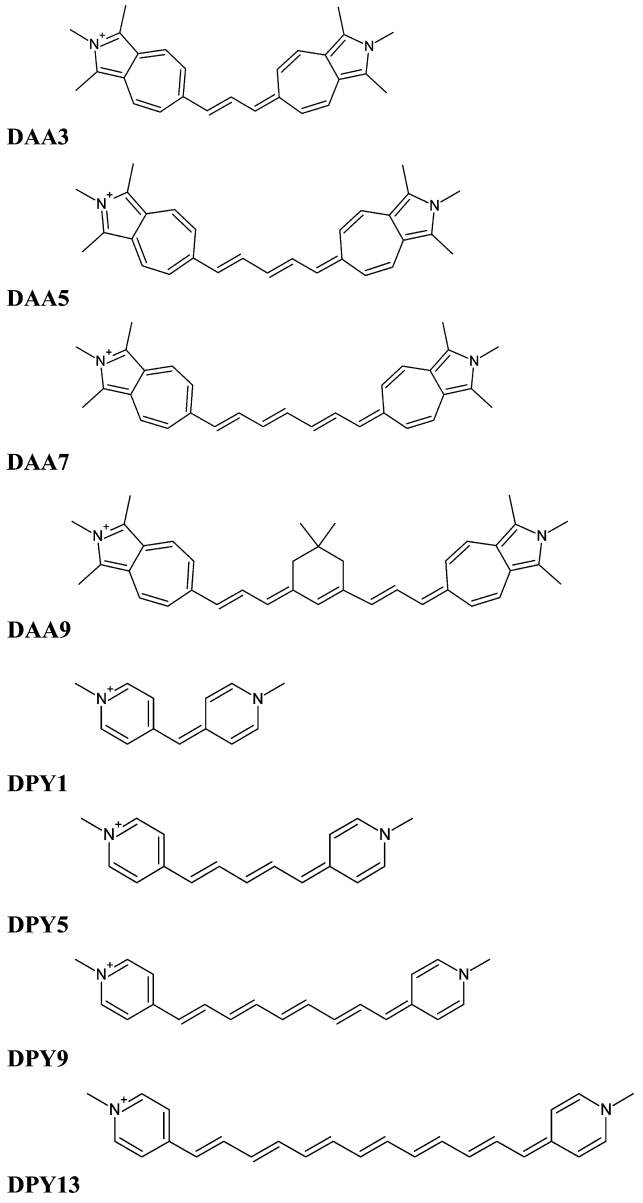

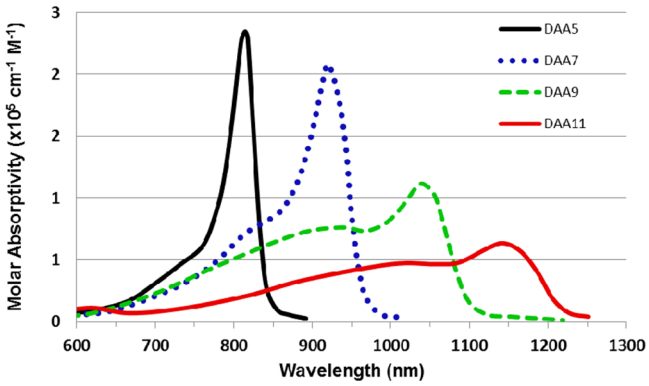

Figure 1. Experimental absorption spectra of DAA*n* chromophores in acetonitrile (adapted from ref 13).

chromism, and the appearance of a new vibrational absorption band corresponding to a C═N bond. However, the line shape of the intermediate length homologue DPY9 (see Figure 2)

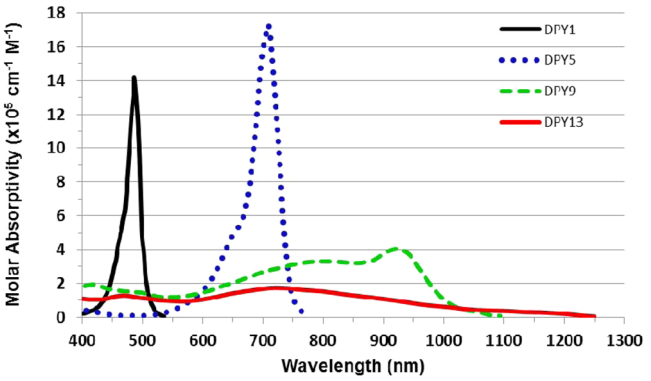

Figure 2. Experimental absorption spectra of DPY*n* chromophores in dimethyl sulfoxide (adapted from ref 17).

combined features of both longer and shorter homologues. This series of compounds was also investigated in the present paper.

To generalize, the sharp absorption band of high intensity is characteristic for the shorter polymethine of symmetric structure, whereas a very broad and low-intensity electronic absorption band was established to be indicative of an asymmetric ground state structure, typical for the longer polymethines. The transition from one type to the other is known as "crossing the cyanine limit". Another confirmation of symmetry-breaking in cyanines was reported by Bouit et al.[17] They demonstrated the gradual crossing of the cyanine limit (absorption band widening) for the same C7 cyanine cation in toluene solution, with the counterions of decreasing size. They also crystallized these cyanine salts and observed an increase in the bond length alternation, reported by the X-ray diffraction. Several authors also identified the effect of the solvent polarity, inducing the symmetry-breaking for cyanines.[18,19] Lepkowicz, Przhonska, and coauthors[20] concluded that a polymethine chain in the ground state may coexist in two charged forms: symmetric and asymmetric; however, the previous computational attempt to identify conditions under which symmetric and asymmetric forms may exist concurrently was not successful:[21] one of two forms was consistently found to be the only energy minimum.

Two empirical models for the cyanine band shapes have been proposed,[22,23] but the first-principles predictions are still rare. To the best of our knowledge, only three band shape predictions have appeared in the literature: one C3 thiacyanine;[24] two C7 indocarbocyanines;[25] and a very detailed study on seven cyanines, C1−C7, with various terminal groups.[26] Although the former papers used exchange-correlation functionals with a larger fraction of Hartree−Fock exchange (BHHLYP and M06-2X) and reproduced the experimental spectra accurately, the latter one used B3LYP and overestimated the molar absorptivity of the lower-energy vibronic band (predicted too sharp peaks as the polymethine chain length increases). In this contribution, we present an improved model that addresses these shortcomings.

Ground state symmetry-breaking in polymethines was studied using both semiempirical and the first-principles methods repeatedly (see the examples in refs 27, 28 and reference therein). Despite the advances in the wave function theory methods, the most accurate theoretical studies of C11 and larger polymethines are limited to the density functional theory (DFT) methods,[29] including time-dependent DFT

DOI: 10.1021/acs.jpca.5b03877
J. Phys. Chem. A XXXX, XXX, XXX−XXX

(TD-DFT).[30] DFT is widely used to make accurate predictions of structure and properties for molecules and solids, including aggregation and crystallization,[31−34] and their emission fingerprints,[35] reaction mechanisms, and reaction rates,[36−38] and linear and nonlinear optical properties.[39−43] A systematic DFT study of the symmetry-breaking in the cyanines was published recently by Yesudas.[44] He emphasized the role of the exchange-correlation functional on crossing the cyanine limit. Specifically, a large fraction of the Hartree−Fock exchange (100%HF, as in M06-HF) was shown to break the symmetry in shorter chains, whereas pure DFT functionals (0%HF, as in BLYP) may never break the ground state symmetry.

In this contribution, we first establish a reliable exchange-correlation functional that describes the cyanine limit in agreement with experiment. Next, we apply it to predict the vibronic structure of the electronic absorption bandshapes. Our working hypothesis is that thermal fluctuations of the solvent reaction field are responsible for the symmetry-breaking of polymethine cations with intermediate chain lengths, which would be symmetric at absolute zero. We propose an implicit solvation model that describes these thermal fluctuations and compares its predictions with experimental spectra.

2. THEORETICAL CONSIDERATIONS AND COMPUTATIONAL DETAILS

2.1. Fluctuations of the Solvent Reaction Field. The solvent effect on the electronic structure of the solute is often described in terms of a polarizable continuum model (PCM),[45] in which solvent is represented implicitly (by mean field approximation) as a uniform medium characterized by a certain dielectric constant. The charge distribution in the solute generates the dielectric response from the solvent, which exerts an external electrostatic potential on the solute (which may be represented, for instance, by a set of charges on the solute surface). This approach became a part of many computer programs under the name of the self-consistent reaction field (SCRF) method. In this work, we use the latest implementation of SCRF in Gaussian 2009, which is called solvent model density (SMD)[46] and includes carefully chosen atomic radii and nonpolar parameters for 184 common solvents. Although explicit treatment of solvent molecules or counterions remains unavoidable in some cases,[40,42,47] the PCM provides implicit treatment of solvent that greatly simplifies the simulation protocol.

We emphasize that the PCM describes the equilibrium situation, and temperature does not enter this model explicitly. The alternative to the reaction field models is presented by a statistical treatment that includes both averages and fluctuation probabilities in the electrostatic potential, electric field, and field gradient exerted by the solvent on the solute.[48] Such a treatment was shown to confirm conclusions of the reaction filed approach while explaining some additional effects beyond mean field approximation.[49] There is experimental evidence to the fact that these fluctuations have a large amplitude, up to 30% of the average. For instance, the solvent electric field produced by the surrounding water molecules on the *N*-methylacetamide is 172 MV/cm, on average, and its root-mean-square fluctuation amplitude is 52 MV/cm.[50] Nonetheless, the computational approaches to account for these filed fluctuations are limited to the explicit solvation models, such as molecular dynamics method.[51]

Here, we introduce an implicit solvation model including field fluctuations. Because the potential and field gradient are centrosymmetric, they will have no effect on symmetry-breaking, and the only electric field fluctuation that will affect the symmetry of the polymethine chain is directed parallel to the chain long axis. In our model, we orient the molecular chain along the z axis by using a Z matrix definition, in which the first and second atoms in this Z matrix are the nearest neighbors of the central atom in the chain. Next, we prepare several (from 10 to 20) systems in the ensemble by applying the finite field in the z direction in steps of 0.0001 atomic units (Gaussian keyword Field=Z-1, Z-2, etc.). The geometry optimization, vibrational analysis, and excited state gradient calculations are then performed for each system in the ensemble independently. The FC line shapes obtained for each of the finite field strengths are then averaged with their Boltzmann weights. These weights are determined from the free energy of the solvated cation combined with the free energy of the solvent fluctuation. The free energy of the solute is determined as coded in Gaussian 09 at the end of vibrational analysis in harmonic approximation. It includes SMD solvation free energy and stabilization by the finite field. The fluctuation free energy, E, is taken in elastic approximation to be quadratically dependent on the finite field, F:

$$E = k \cdot F^2$$

Here, k is elastic (Hooke's) constant. It and the line-broadening Γ are the only two adjustable parameters of the model (specific for a given solvent). In addition, we also rescale the resulting spectra to match experimental absorbance at the maximum.

2.2. Details of Quantum Chemical Calculations. The ground state geometry and normal-mode analysis as well as the excited state single-point energy gradient calculations were performed using the Gaussian 2009 suite of programs.[52] DFT with the SOGGA11-X exchange-correlation functional[53] was chosen for the reasons explained below. The D95 basis set[54] with no diffuse functions was selected to prevent the artificial Rydberg mixing into the valence excited states, as described in refs 55 and 56. Geometry optimizations were performed without any symmetry constraints in solvent (acetonitrile for DAA*n*, and dimethilsulfoxide for DPY*n* series of chromophores) for the meaningful comparison with experimental spectra.

TD-DFT[57] was used to describe the singlet excited states, their electron densities, and energy gradients. A nonequilibrium solvation model was used in recognition of the fact that solvent relaxation is much slower than the absorption process. We choose not to optimize the excited state geometry because this procedure is not straightforward when the state crossing occurs or when CC torsional angles twist.[58,59] The use of the vertical excitation energy, combined with excited state gradients and harmonic approximation, produced the adiabatic excitation energy internally in KTS code. The prediction of the vertical excitation energy in polymethines deserves more detailed consideration.

The lowest excitation energies in polymethines are known to present a challenge for theoretical prediction. The static (time-independent) DFT, also known as ΔSCF,[60] was probably the oldest method applied to study excitation energies in polymethines. When combined with local exchange-correlation functionals, it underestimated the absolute energies of merocyanine dyes, but well reproduced the solvatochromic shift (fairly large in this case).[61] Yet when used with the hybrid functional, the cyanine excitation energy was reproduced accurately.[62] The time-dependent DFT (with both pure and

DOI: 10.1021/acs.jpca.5b03877
J. Phys. Chem. A XXXX, XXX, XXX−XXX

hybrid functionals) strongly (0.5−1 eV) overestimated the excitation energies,[63] which made them unique among other types of chromophores. A more advanced complete-active-space perturbation theory of the second order (CASPT2), applied to the simplest cyanines (with NH_2 terminal groups), demonstrated a better agreement with experimental data when compared with the predictions of the single-reference TD-DFT methods.[64] This was misinterpreted as evidence of the multiconfigurational character of the lowest excited state in cyanines, even though the CASPT2 wave function analysis indicated this state to be predominantly HOMO−LUMO excitation.

More recent CASPT2 studies by Sent et al.[65] employed an advanced ionization potential electron affinity shift procedure for the zero-order Hamiltonian and increased the best estimates for excitation energies by ∼0.2 eV (closer to TD-DFT predicted values). These predicted gas phase vertical excitation energies were in close agreement with other correlated wave function calculations: extrapolated approximate coupled cluster singles, doubles, and triples (exCC3) and by diffusion Monte Carlo (DMC). Considering nontrivial evaluation of the solvent effects on the cyanine absorption spectra (subject of the present study), these theoretical gas phase estimates became a reliable benchmark. Although wave function theory methods are prohibitively expensive in applications to larger polymethines, less expensive first-principle methods had been applied to test their performance.

A series of papers by Jacquemin et al.[66−70] unfolded like chapters in a mystery novel: in 2010, they admitted that all TD-DFT methods showed "dreadful" performances for cyanine dyes;[66] in 2012, they reversed their verdict to "not guilty";[67] in 2014, they declared that the Bethe−Salpeter approach (a post-DFT perturbation treatment originating from solid state theory) "demonstrates, for the first time, that one can accurately restore cyanine transition energies with an ab initio method computationally tractable for large compounds ... significantly different from the TD-DFT results".[68,69] Yet, in 2015, they find a SOS-CIS(D)/TD-DFT hybrid method to be both accurate and consistent.[70] Improvements of various degrees were also reported with the use of optimal tuning in range-separated functionals,[71,72] double-hybrid B2PLYP (including a fraction of MP2 correlation),[73] the restricted spin ensemble Kohn−Sham approach,[74] and spin−flip DFT (SF-DFT).[75]

Meanwhile, one of us traced[76] the source of inaccuracies in adiabatic TD-DFT for the polymethine case to the underlying assumption that excited state energy is evaluated in the potential, generated by the ground state density. When the charge redistribution upon the excitation is large (in the case of polymethines, it is even to odd atoms charge transfer), the performance suffers. To mitigate this, it was proposed[76] to use static DFT to evaluate the energies on the excited state densities, obtained with TD-DFT. This approach was classified as CV(4) in a more general framework of constricted variational methods.[77] It was used successfully to correct TD-DFT inaccuracies in excitation energy predictions for squaraines,[9,10] cyanines,[76] coordination complexes,[78] and higher lying excited states in *para*-nitroaniline.[79] Here call this a frozen density DFT method (FD-DFT), use the SOGGA11-X functional to produce the ground and excited state densities, and the B3LYP functional to evaluate their energies in a single step (with no SCF convergence), then apply a spin-purification formula to extract the singlet energy from the open shell determinant energies ($E_S = 2E_{\uparrow\downarrow} - E_{\uparrow\uparrow}$).

2.3. Details of Franck−Condon Calculations. The vibronic structure of electronic absorption spectra were predicted using the Franck−Condon approximation with linear electron−phonon coupling as implemented in the KTS program.[80−83] The program implements time-domain formalism[84,85] and a multimode shifted harmonic oscillator model similar to that developed in Orca_ASA.[86,87] Linear coupling means that the Hessians of the initial and final states are assumed to be the same, which makes KTS computationally inexpensive. The input data consists of the ground state normal mode vectors and frequencies as well as the vertical excitation energies and excited state gradients calculated in the geometry of the ground state. These data sets are prepared by parsing Gaussian 2009 output files. The line shape is then calculated through the Fourier transform of the generating function, expressed as a sum over per-mode dimensionless Huang−Rhys parameters (see refs 81−83 for details). The method does not allow any limitations on the maximum number of overtones or combination bands.

To counteract the formal divergence of the Fourier integral, the exponential damping is introduced, and integration is restricted to a large time interval of $\pm 2 \times 10^5$ a.u. (4.5 ps). Introduction of exponential damping is equivalent to convolution of the entire spectrum with a Lorentzian of the width Γ. It is expressed in atomic units: $\Gamma = 10^{-5}$ a.u. corresponds to fwhm = 2.7×10^{-4} eV. This procedure is sometimes considered as a phenomenological method to account for the homogeneous line-broadening.[88] In this work. we treat Γ as a solvent-specific empirical parameter that determines the resolution of the calculated vibronic bands.

3. RESULTS AND DISCUSSION

For the delicate spectral predictions to be accurate, it is critically important to choose the level of theory, which reproduces the experimentally found crossing of cyanine limit. From the data, presented in Figures 1 and 2, we know that in DPY13, the ground state symmetry is broken while DDA11 is still symmetric. We used this information to verify some of the exchange-correlation functionals available in Gaussian. We selected the small (<1D) dipole moment in the *z*-direction as the criterion for the molecular structure to be symmetric. The single most important property of the exchange-correlation functional is the fraction of Hartree−Fock exchange (%HF). Our calculations found that TPSSh[89] (10%HF), tHCTHhyb[90] (15%HF), B3LYP[91] (20%HF), PBE0[92] (25%HF), and M05-QX[93] (35%HF) all incorrectly predicted DPY13 to be symmetric. At the same time, M06-HF[94] (100%HF), M06-2X[95] (54%HF), and BMK[96] (42%HF) incorrectly predicted symmetry-breaking in DDA11. We were able to identify only one global hybrid functional that was satisfactory by both of our criteria: SOGGA11-X[97] (40%HF). It is worth noting that the electronic structure of the cyanine cations is very sensitive to overdelocalization, expected from HF exchange: a minor increase in the fraction of HF exchange from 40% to 42% (BMK) results in crossing the cyanine limit for DDA11, in clear disagreement with experiment.

With this exchange-correlation functional, selected as the most appropriate for the task, we predicted the line shapes for DPY*n* series without the external field. Although DPY1 and DPY5 spectra were predicted to be sharp peaks (in close agreement with Figure 1), DPY13 was found to have a wide

DOI: 10.1021/acs.jpca.5b03877
J. Phys. Chem. A XXXX, XXX, XXX−XXX

and low bell shape with a flat top (again in close agreement with Figure 1). Disagreement was observed, however, in the case of DPY9: our calculations predicted a sharp peak with an insignificant short wavelength shoulder.

Next, the finite field of the variable strengths was applied to DPY9. The changes in the absorption band were dramatic (Figure 3). Although the weak field of 0.0001 au had almost no

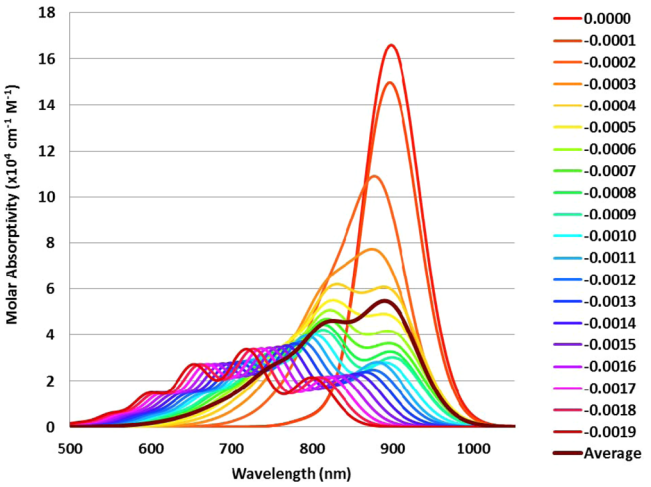

Figure 3. Predicted absorption spectra of the chromophore DPY9 under the external electric field applied along the N..N molecular axis with strengths of 0.0001−0.0019 atomic units.

effect on the line shape, the single peak remained sharp, indicative of a small geometry change upon the electronic excitation, a typical situation for symmetric cyanine. The fields of 0.0002 and 0.0003 resulted in the appearance of a short wavelength shoulder. At the field of 0.0004, the double peak appeared, and fields of 0.0009 and over produced a clear vibronic structure of three or more peaks. This is indicative of the cyanine limit crossing. The finite field also resulted in a blue shift of the vertical excitation energy (~0.02 eV or 10 nm for each field increment). As a result, after the Boltzmann averaging, the vibronic structure is lost, and the shape becomes a single peak with a shoulder and a tail, extending 300 nm to the blue. For this polar solvent (dimethyl sulfoxide), the best fluctuation elastic constant and line width parameter that reproduced the experimental line shapes were found to be 4.5 × 10^6 kcal/mol·a.u.^{2} and 1.2 × 10^{-3} a.u., respectively. The Boltzmann weights appear to be nearly evenly distributed between 4% for the field of both 0 and 0.0012 atomic units and reaching 11% toward the middle of this range. When a similar procedure is applied to the other DPY*n* chromophores, the trends remain the same while the changes are less dramatic (Figure 4). As one can see, all four spectra are now in qualitative agreement with the experimental ones presented in Figure 2.

Finally, we applied the same procedure to four chromophores in the DAA*n* series (Figure 5), and obtained qualitative agreement with experimental spectra (Figure 1). For the less polar solvent (acetonitrile), the fluctuation elastic constant, *k*, and line width parameter, Γ, that reproduced the experimental line shapes were found to be 1.0 × 10^7 kcal/mol·a.u.^{2} and 8.4 × 10^{-4} a.u., respectively. Just as in the DPY*n* series, the two shorter-chain members with very stable symmetric structures demonstrated sharp peaks; however, this time, both longer chain members approach the cyanine limit so that their

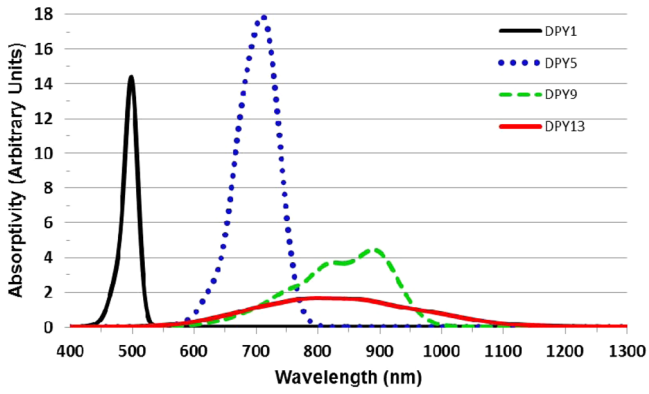

Figure 4. Predicted absorption spectra of the chromophores in the DPY*n* series, obtained as Boltzmann average of the shapes obtained under the external electric fields.

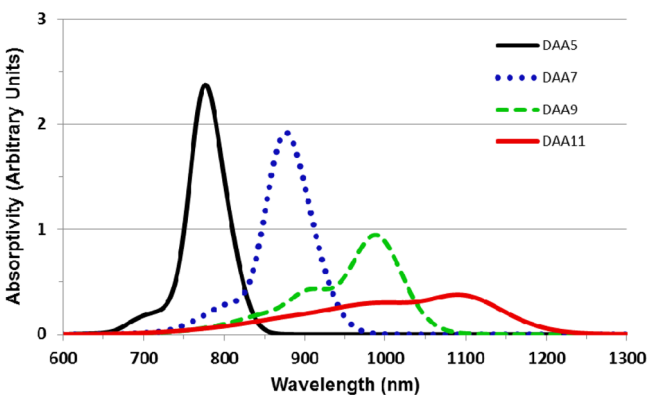

Figure 5. Predicted absorption spectra of the chromophores in DAA*n* series, obtained as a Boltzmann average of the shapes, obtained under the external electric fields.

symmetry can be easily broken by the solvent reaction field fluctuations. This resulted in the wide shoulders and the tails that extend hundreds of nanometers to the blue.

It is worth noting that the agreement with experiment is obtained without an empirical energy shift or any energy-fitting parameters. The success of the spectral predictions are due in part to the FD-DFT method that performs rather well for the vertical transition energies. The vertical excitation energy predictions are collected in Table 1, together with TD-DFT results. Both experimental and FC-predicted λ_{max} are rather close to the vertical FD-DFT predictions in all cases, except for DPY13. One can see from Table 1 that TD-DFT predictions are systematically in error by nearly 0.5 eV (up to 350 nm), which is consistent with the previous reports.[64,66] The FD-DFT predictions, on the other hand, are accurate to <0.1 eV (and 25−50 nm). The DPY13 anomaly could be successfully predicted only after the ensemble averaging over the electric field fluctuations, as well as the spectral shapes of DAA7, DAA9, and DPY9.

4. CONCLUSIONS

We have confirmed the hypothesis that the asymmetric form of cyanines can coexist with their symmetric form in solution only due to the thermal fluctuations of solvent reaction field. We also propose a numerical model, taking these fluctuations into account, and based on the first principle calculations. This model is an extension of a polarizable continuum model

DOI: 10.1021/acs.jpca.5b03877
J. Phys. Chem. A XXXX, XXX, XXX−XXX

Table 1. Predicted and Experimental Absorption Maxima (λ, nm) and Vertical Excitation Energies (ΔE, eV)[a]s

	DAA5	DAA7	DAA9	DAA11	DPY1	DPY5	DPY9	DPY11
λ_{max}, experimental	814[b]	921[b]	1040[b]	1143[b]	488[c]	709[c]	925[c]	739[c]
ΔE_{max}, experimental	1.52	1.35	1.19	1.08	2.54	1.75	1.34	1.68
λ_{max}, FD-DFT	780	880	995	1096	497	715	895	795
ΔE_{max}, FD-DFT	1.59	1.41	1.25	1.13	2.49	1.73	1.39	1.56
$\lambda_{vertical}$, FD-DFT	795	899	992	1078	494	717	899	1069
$\Delta E_{vertical}$, FD-DFT	1.56	1.38	1.25	1.15	2.51	1.73	1.38	1.16
$\lambda_{vertical}$, TD-DFT	603	672	738	801	395	548	675	800
$\Delta E_{vertical}$, TD-DFT	2.06	1.85	1.68	1.55	3.14	2.26	1.84	1.55

[a]The vertical excitation energy predictions are made with habitual adiabatic TD-DFT and with FD-DFT. Predictions of λ_{max} involved multiple finite field calculations and ensemble averaging. See text for details. [b]Ref 13. [c]Ref 17.

(PCM) to the finite temperatures. The only two empirical parameters of this model (fluctuation elastic constant and line width parameter) are specific for each solvent and should, in principle, be optimized together with PCM parameters. In principle, this polarizable continuum model with fluctuations (PCMF), can be used to study thermochromics effects. This work is presently under way.

The shorter-chain polymethines (DPY1, DPY5, DAA5, DAA7) are relatively stable in their symmetric forms, and their spectra are not significantly affected by the solvent reaction field fluctuations. The longer polymethines that approach the cyanine limit (DPY9, DAA9, DAA11) demonstrate that their symmetry can be easily perturbed. For those polymethines, the spectral shapes are predicted correctly for the first time by a combination of DFT methods with PCMF. These spectral shapes include the maximum, short-wavelength shoulder, and ~300 nm tail. We emphasize the critical importance of the exchange-correlation functional to describe the delicate balance between symmetric and perturbed forms. Out of the wide range of the global hybrid functionals considered in this work, only SOGGA11-X seemed to achieve this delicate balance. This work can be considered as proof of principle, and further fine-tuning is clearly needed for both solvent-specific parameters and an exchange-correlation functional before PCMF can be recommended for routine investigations.

AUTHOR INFORMATION

Corresponding Author

*Phone: 1-407-374-3783. E-mail: amasunov@ucf.edu.

Notes

The authors declare no competing financial interest.

ACKNOWLEDGMENTS

This work was supported by the Russian Science Foundation, Contract No. 14−43−00052. The authors acknowledge the National Energy Research Scientific Computing Center (NERSC), and the University of Central Florida Advanced Research Computing Center (https://arcc.ist.ucf.edu) for providing computational resources and support. A.Y.F. and A.E.M. thank Dr. A. V. Scherbinin (Moscow State University) for making the KTS program package available.

DEDICATION

The article is dedicated to the memory of Dr. Olga Viktorovna Przhonska (1946−2014) and her lifelong accomplishments in spectroscopic studies of polymethine dyes.

REFERENCES

(1) Ishchenko, A. A. Laser Media Based on Polymethine Dyes. *Quantum Electron.* **1994**, *24*, 471−492.
(2) Hany, R.; Fan, B.; de Castro, F. A.; Heier, J.; Kylberg, W.; Nuesch, F. Strategies to Improve Cyanine Dye Multi Layer Organic Solar Cells. *Prog. Photovoltaics* **2011**, *19*, 851−857.
(3) Bulavko, G. V.; Ishchenko, A. A. Organic Bulk Heterojunction Photovoltaic Structures: Design, Morphology and Properties. *Russ. Chem. Rev.* **2014**, *83*, 575−599.
(4) Zitzler-Kunkel, A.; Lenze, M. R.; Kronenberg, N. M.; Krause, A.-M.; Stolte, M.; Meerholz, K.; Wuerthner, F. NIR-Absorbing Merocyanine Dyes for BHJ Solar Cells. *Chem. Mater.* **2014**, *26*, 4856−4866.
(5) Seo, S.; Pascal, S.; Park, C.; Shin, K.; Yang, X.; Maury, O.; Sarwade, B. D.; Andraud, C.; Kim, E. NIR Electrochemical Fluorescence Switching from Polymethine Dyes. *Chem. Sci.* **2014**, *5*, 1538−1544.
(6) James, N. S.; Chen, Y.; Joshi, P.; Ohulchanskyy, T. Y.; Ethirajan, M.; Henary, M.; Strekowsk, L.; Pandey, R. K. Evaluation of Polymethine Dyes as Potential Probes for Near Infrared Fluorescence Imaging of Tumors: Part-1. *Theranostics* **2013**, *3*, 692−702.
(7) Gustafson, T. P.; Cao, Q.; Achilefu, S.; Berezin, M. Y. Defining a Polymethine Dye for Fluorescence Anisotropy Applications in the Near-Infrared Spectral Range. *ChemPhysChem* **2012**, *13*, 716−723.
(8) Hales, J. M.; Matichak, J.; Barlow, S.; Ohira, S.; Yesudas, K.; Bredas, J.-L.; Perry, J. W.; Marder, S. R. Design of Polymethine Dyes with Large Third-Order Optical Nonlinearities and Loss Figures of Merit. *Science* **2010**, *327*, 1485−1488.
(9) Peceli, D.; Hu, H.; Fishman, D. A.; Webster, S.; Przhonska, O. V.; Kurdyukov, V. V.; Slominsky, Y. L.; Tolmachev, A. I.; Kachkovski, A. D.; Gerasov, A. O.; Masunov, A. E. et, a. Enhanced Intersystem Crossing Rate in Polymethine-Like Molecules: Sulfur-Containing Squaraines versus Oxygen-Containing Analogues. *J. Phys. Chem. A* **2013**, *117*, 2333−2346.
(10) Moreshead, W. V.; Przhonska, O. V.; Bondar, M. V.; Kachkovski, A. D.; Nayyar, I. H.; Masunov, A. E.; Woodward, A. W.; Belfield, K. D. Design of a New Optical Material with Broad Spectrum Linear and Two-Photon Absorption and Solvatochromism. *J. Phys. Chem. C* **2013**, *117*, 23133−23147.
(11) Hu, H.; Fishman, D. A.; Gerasov, A. O.; Przhonska, O. V.; Webster, S.; Padilha, L. A.; Peceli, D.; Shandura, M.; Kovtun, Y. P.; Kachkovski, A. D.; Nayyar, I. H.; Masunov, A. E. et, a. Two-Photon Absorption Spectrum of a Single Crystal Cyanine-Like Dye. *J. Phys. Chem. Lett.* **2012**, *3*, 1222−1228.
(12) Webster, S.; Peceli, D.; Hu, H.; Padilha, L. A.; Przhonska, O. V.; Masunov, A. E.; Gerasov, A. O.; Kachkovski, A. D.; Slominsky, Y. L.; Tolmachev, A. I. et, a. Near-Unity Quantum Yields for Intersystem Crossing and Singlet Oxygen Generation in Polymethine-like Molecules: Design and Experimental Realization. *J. Phys. Chem. Lett.* **2010**, *1*, 2354−2360.
(13) Przhonska, O. V.; Hu, H.; Webster, S.; Bricks, J. L.; Viniychuk, A. A.; Kachkovski, A. D.; Slominsky, Y. L. Electronic Transitions in a Series of 2-Azaazulene Polymethine Dyes with Different pi-Conjugation Lengths. *Chem. Phys.* **2013**, *411*, 17−25.

DOI: 10.1021/acs.jpca.5b03877
J. Phys. Chem. A XXXX, XXX, XXX−XXX

(14) Tolbert, L. M.; Zhao, X. D. Beyond the Cyanine Limit: Peierls Distortion and Symmetry Collapse in a Polymethine Dye. *J. Am. Chem. Soc.* **1997**, *119*, 3253−3258.
(15) Su, W. P.; Schrieffer, J. R.; Heeger, A. J. Soliton Excitations In Polyacetylene. *Phys. Rev. B: Condens. Matter Mater. Phys.* **1980**, *22*, 2099−2111.
(16) Reimers, J. R.; Hush, N. S. The Effects of Couplings to Symmetric and Antisymmetric Modes and Minor Asymmetry on the Spectral Properties of Mixed-Valence and Related Charge-Transfer Systems. *Chem. Phys.* **1996**, *208*, 177−193.
(17) Bouit, P.-A.; Aronica, C.; Toupet, L.; Le Guennic, B.; Andraud, C.; Maury, O. Continuous Symmetry Breaking Induced by Ion Pairing Effect in Heptamethine Cyanine Dyes: Beyond the Cyanine Limit. *J. Am. Chem. Soc.* **2010**, *132*, 4328−4335.
(18) Avdeeva, V. I.; Alperovich, M. A.; Babenko, V. A.; Levkoev, II; Malyshev, V. I.; Sychev, A. A.; Shibanov, A. N. Effect of Solvation on Spectroscopic Properties of Pentacarbocyanine Dye Solutions used in Neodymium-Glass Lasers. *Kvantovaya Elektron.* **1975**, *2*, 540−545.
(19) Ishchenko, A. A.; Derevyanko, N. A.; Zubarovskii, V. M.; Tolmachev, A. I. Influence of Length of the Polymethine Chain on Width of Absorption Bands of Symmetric Cyanine Dyes. *Theor. Exp. Chem.* **1985**, *20*, 415−422.
(20) Lepkowicz, R. S.; Przhonska, O. V.; Hales, J. M.; Fu, J.; Hagan, D. J.; Van Stryland, E. W.; Bondar, M. V.; Slominsky, Y. L.; Kachkovski, A. D. Nature of the Electronic Transitions in Thiacarbocyanines with a Long Polymethine Chain. *Chem. Phys.* **2004**, *305*, 259−270.
(21) Iordanov, T. D.; Davis, J. L.; Masunov, A. E.; Levenson, A.; Przhonska, O. V.; Kachkovski, A. D. Symmetry Breaking in Cationic Polymethine Dyes, Part 1: Ground State Potential Energy Surfaces and Solvent Effects on Electronic Spectra of Streptocyanines. *Int. J. Quantum Chem.* **2009**, *109*, 3592−3601.
(22) Terenziani, F.; Przhonska, O. V.; Webster, S.; Padilha, L. A.; Slominsky, Y. L.; Davydenko, I. G.; Gerasov, A. O.; Kovtun, Y. P.; Shandura, M. P.; Kachkovski, A. D.; Hagan, D. J.; Van Stryland, E. W.; Painelli, A. Essential-State Model for Polymethine Dyes: Symmetry Breaking and Optical Spectra. *J. Phys. Chem. Lett.* **2010**, *1*, 1800−1804.
(23) Egorov, V. V. Optical Lineshapes for Dimers of Polymethine Dyes: Dozy-Chaos Theory of Quantum Transitions and Frenkel Exciton Effect. *RSC Adv.* **2013**, *3*, 4598−4609.
(24) Guillaume, M.; Liegeois, V.; Champagne, B.; Zutterman, F. Time-Dependent Density Functional Theory Investigation of the Absorption and Emission Spectra of a Cyanine Dye. *Chem. Phys. Lett.* **2007**, *446*, 165−169.
(25) Pascal, S.; Haefele, A.; Monnereau, C.; Charaf-Eddin, A.; Jacquemin, D.; Le Guennic, B.; Andraud, C.; Maury, O. Expanding the Polymethine Paradigm: Evidence for the Contribution of a Bis-Dipolar Electronic Structure. *J. Phys. Chem. A* **2014**, *118*, 4038−4047.
(26) Lin, K. T. H.; Silzel, J. W. Relation of Molecular Structure to Franck-Condon Bands in the Visible-Light Absorption Spectra of Symmetric Cationic Cyanine Dyes. *Spectrochim. Acta, Part A* **2015**, *142*, 210−219.
(27) Fabian, J. Symmetry-Lowering Distortion of Near-Infrared Polymethine Dyes - a Study by First-Principles Methods. *J. Mol. Struct.: THEOCHEM* **2006**, *766*, 49−60.
(28) Kachkovski, O. D.; Tolmachov, O. I.; Slominskii, Y. L.; Kudinova, M. O.; Derevyanko, N. O.; Zhukova, O. O. Electronic Properties of Polymethine Systems 7: Soliton Symmetry Breaking and Spectral Features of Dyes with a Long Polymethine Chain. *Dyes Pigm.* **2005**, *64*, 207−216.
(29) Gill, P. M. W. Obituary: Density Functional Theory (1927−1993). *Aust. J. Chem.* **2001**, *54*, 661−662.
(30) Adamo, C.; Jacquemin, D. The Calculations of Excited-State Properties with Time-Dependent Density Functional Theory. *Chem. Soc. Rev.* **2013**, *42*, 845−856.
(31) Liu, J.; Mikhaylov, I. A.; Zou, J.; Osaka, I.; Masunov, A. E.; McCullough, R. D.; Zhai, L. Insight into How Molecular Structures of Thiophene-Based Conjugated Polymers Affect Crystallization Behaviors. *Polymer* **2011**, *52*, 2302−2309.
(32) Cardenas-Jiron, G. I.; Masunov, A.; Dannenberg, J. J. Molecular Orbital Study of Crystalline p-Benzoquinone. *J. Phys. Chem. A* **1999**, *103*, 7042−7046.
(33) Passier, R.; Ritchie, J. P.; Toro, C.; Diaz, C.; Masunov, A. E.; Belfield, K. D.; Hernandez, F. E. Thermally Controlled Preferential Molecular Aggregation State in a Thiacarbocyanine Dye. *J. Chem. Phys.* **2010**, *133*, 1345081−134508.
(34) Masunov, A. E.; Zorkii, P. M. Geometric Characteristics of Halogen-Halogen Intermolecular Contacts in Organic-Crystals. *Zh. Fiz. Khim.* **1992**, *66*, 60−69.
(35) Crotty, A. M.; Gizzi, A. N.; Rivera-Jacquez, H. J.; Masunov, A. E.; Hu, Z.; Geldmeier, J. A.; Gesquiere, A. J. Molecular Packing in Organic Solar Cell Materials: Insights from the Emission Line Shapes of P3HT/PCBM Polymer Blend Nanoparticles. *J. Phys. Chem. C* **2014**, *118*, 19975−19984.
(36) Patel, P. D.; Masunov, A. E. Theoretical Study of Photochromic Compounds: Part 3. Prediction of Thermal Stability. *J. Phys. Chem. C* **2011**, *115*, 10292−10297.
(37) Ignatov, S. K.; Gadzhiev, O. B.; Razuvaev, A. G.; Masunov, A. E.; Schrems, O. Adsorption of Glyoxal (CHOCHO) and Its UV Photolysis Products on the Surface of Atmospheric Ice Nanoparticles. DFT and Density Functional Tight-Binding Study. *J. Phys. Chem. C* **2014**, *118*, 7398−7413.
(38) Gadzhiev, O. B.; Ignatov, S. K.; Krisyuk, B. E.; Maiorov, A. V.; Gangopadhyay, S.; Masunov, A. E. Quantum Chemical Study of the Initial Step of Ozone Addition to the Double Bond of Ethylene. *J. Phys. Chem. A* **2012**, *116*, 10420−10434.
(39) Kauffman, J. F.; Turner, J. M.; Alabugin, I. V.; Breiner, B.; Kovalenko, S. V.; Badaeva, E. A.; Masunov, A.; Tretiak, S. Two-Photon Excitation of Substituted Enediynes. *J. Phys. Chem. A* **2006**, *110*, 241−251.
(40) De Boni, L.; Toro, C.; Masunov, A. E.; Hernandez, F. E. Untangling the Excited States of DR1 in Solution: an Experimental and Theoretical Study. *J. Phys. Chem. A* **2008**, *112*, 3886−3890.
(41) Belfield, K. D.; Bondar, M. V.; Morales, A. R.; Yue, X.; Luchita, G.; Przhonska, O. V.; Kachkovsky, O. D. Two-Photon Absorption and Time-Resolved Stimulated Emission Depletion Spectroscopy of a New Fluorenyl Derivative. *ChemPhysChem* **2012**, *13*, 3481−3491.
(42) Belfield, K. D.; Bondar, M. V.; Frazer, A.; Morales, A. R.; Kachkovsky, O. D.; Mikhailov, I. A.; Masunov, A. E.; Przhonska, O. V. Fluorene-Based Metal-Ion Sensing Probe with High Sensitivity to Zn2+ and Efficient Two-Photon Absorption. *J. Phys. Chem. B* **2010**, *114*, 9313−9321.
(43) Belfield, K. D.; Bondar, M. V.; Hernandez, F. E.; Masunov, A. E.; Mikhailov, I. A.; Morales, A. R.; Przhonska, O. V.; Yao, S. Two-Photon Absorption Properties of New Fluorene-Based Singlet Oxygen Photosensitizers. *J. Phys. Chem. C* **2009**, *113*, 4706−4711.
(44) Yesudas, K. Cationic Cyanine Dyes: Impact of Symmetry-Breaking on Optical Absorption and Third-Order Polarizabilities. *Phys. Chem. Chem. Phys.* **2013**, *15*, 19465−19477.
(45) Cramer, C. J.; Truhlar, D. G. Implicit Solvation Models: Equilibria, Structure, Spectra, and Dynamics. *Chem. Rev.* **1999**, *99*, 2161−2200.
(46) Marenich, A. V.; Cramer, C. J.; Truhlar, D. G. Universal Solvation Model Based on Solute Electron Density and on a Continuum Model of the Solvent Defined by the Bulk Dielectric Constant and Atomic Surface Tensions. *J. Phys. Chem. B* **2009**, *113*, 6378−6396.
(47) Masunov, A.; Tretiak, S.; Hong, J. W.; Liu, B.; Bazan, G. C. Theoretical Study of the Effects of Solvent Environment on Photophysical Properties and Electronic Structure of Paracyclophane Chromophores. *J. Chem. Phys.* **2005**, *122*, 2245051−2245057.
(48) Karlstrom, G.; Halle, B. A Fluctuation Approach To Solvation In Polar Fluids. *J. Chem. Phys.* **1993**, *99*, 8056−8062.
(49) Stenhammar, J.; Linse, P.; Karlstrom, G. A Unified Treatment of Polar Solvation using Electrostatic Fluctuations. *Chem. Phys. Lett.* **2011**, *501*, 364−368.
(50) Lee, H.; Lee, G.; Jeon, J.; Cho, M. Vibrational Spectroscopic Determination of Local Solvent Electric Field, Solute-Solvent

DOI: 10.1021/acs.jpca.5b03877
J. Phys. Chem. A XXXX, XXX, XXX−XXX

Electrostatic Interaction Energy, and Their Fluctuation Amplitudes. *J. Phys. Chem. A* **2012**, *116*, 347−357.
(51) Fried, S. D.; Wang, L.-P.; Boxer, S. G.; Ren, P.; Pande, V. S. Calculations of the Electric Fields in Liquid Solutions. *J. Phys. Chem. B* **2013**, *117*, 16236−16248.
(52) Frisch, M. J.; Trucks, G. W.; Schlegel, H. B.; Scuseria, G. E.; Robb, M. A.; Cheeseman, J. R.; Scalmani, G.; Barone, V.; Mennucci, B.; Petersson, G. A.; et al. *Gaussian 09, Rev. D.01*; Gaussian, Inc.: Wallingford, CT, 2009.
(53) Peverati, R.; Truhlar, D. G. Communication: A Global Hybrid Generalized Gradient Approximation to the Exchange-Correlation Functional that Satisfies the Second-Order Density-Gradient Constraint and has Broad Applicability in Chemistry. *J. Chem. Phys.* **2011**, *135*, 1911021−1911025.
(54) Dunning, T. H.; Hay, P. J. *Modern Theoretical Chemistry*; Schaefer, H. F., III, Ed.; Springer US: Boston, MA, 1977; Vol. 3; pp 1−21.
(55) Nayyar, I. H.; Masunov, A. E.; Tretiak, S. Comparison of TD-DFT Methods for the Calculation of Two-Photon Absorption Spectra of Oligophenylvinylenes. *J. Phys. Chem. C* **2013**, *117*, 18170−18189.
(56) Masunov, A. E.; Mikhailov, I. A. Theory and Computations of Two-Photon Absorbing Photochromic Chromophores. *Eur. J. Chem.* **2010**, *1*, 142−161.
(57) Casida, M. E.; Huix-Rotllant, M. Progress in Time-Dependent Density-Functional Theory. *Annu. Rev. Phys. Chem.* **2012**, *63*, 287−323.
(58) Freidzon, A. Y.; Safonov, A. A.; Bagaturyants, A. A.; Alfimov, M. V. Solvatofluorochromism and Twisted Intramolecular Charge-Transfer State of the Nile Red Dye. *Int. J. Quantum Chem.* **2012**, *112*, 3059−3067.
(59) Dietzek, B.; Pascher, T.; Yartsev, A. Tracking Ultrafast Excited-State Bond-Twisting Motion in Solution Close to the Franck-Condon Point. *J. Phys. Chem. B* **2007**, *111*, 6034−6041.
(60) Ziegler, T.; Rauk, A.; Baerends, E. J. Calculation of Multiplet Energies by Hartree-Fock-Slater Method. *Theor. Chim. Acta* **1977**, *43*, 261−271.
(61) Toutchkine, A.; Han, W.-G.; Ullmann, M.; Liu, T.; Bashford, D.; Noodleman, L.; Hahn, K. M. Experimental and DFT Studies: Novel Structural Modifications Greatly Enhance the Solvent Sensitivity of Live Cell Imaging Dyes. *J. Phys. Chem. A* **2007**, *111*, 10849−10860.
(62) Kowalczyk, T.; Yost, S. R.; Van Voorhis, T. Assessment of the Delta SCF Density Functional Theory Approach for Electronic Excitations in Organic Dyes. *J. Chem. Phys.* **2011**, *134*, 0541281−0541288.
(63) Fabian, J. TDDFT Calculations of Vis/NIR Absorbing Compounds. *Dyes Pigm.* **2010**, *84*, 36−53.
(64) Schreiber, M.; Buss, V.; Fulscher, M. P. The Electronic Spectra of Symmetric Cyanine Dyes: A CASPT2 Study. *Phys. Chem. Chem. Phys.* **2001**, *3*, 3906−3912.
(65) Send, R.; Valsson, O.; Filippi, C. Electronic Excitations of Simple Cyanine Dyes: Reconciling Density Functional and Wave Function Methods. *J. Chem. Theory Comput.* **2011**, *7*, 444−455.
(66) Jacquemin, D.; Perpete, E. A.; Ciofini, I.; Adamo, C.; Valero, R.; Zhao, Y.; Truhlar, D. G. On the Performances of the M06 Family of Density Functionals for Electronic Excitation Energies. *J. Chem. Theory Comput.* **2010**, *6*, 2071−2085.
(67) Jacquemin, D.; Zhao, Y.; Valero, R.; Adamo, C.; Ciofini, I.; Truhlar, D. G. Verdict: Time-Dependent Density Functional Theory "Not Guilty" of Large Errors for Cyanines. *J. Chem. Theory Comput.* **2012**, *8*, 1255−1259.
(68) Boulanger, P.; Jacquemin, D.; Duchemin, I.; Blase, X. Fast and Accurate Electronic Excitations in Cyanines with the Many-Body Bethe-Salpeter Approach. *J. Chem. Theory Comput.* **2014**, *10*, 1212−1218.
(69) Boulanger, P.; Chibani, S.; Le Guennic, B.; Duchemin, I.; Blase, X.; Jacquemin, D. Combining the Bethe-Salpeter Formalism with Time-Dependent DFT Excited-State Forces to Describe Optical Signatures: NBO Fluoroborates as Working Examples. *J. Chem. Theory Comput.* **2014**, *10*, 4548−4556.
(70) Le Guennic, B.; Jacquemin, D. Taking up the Cyanine Challenge with Quantum Tools. *Acc. Chem. Res.* **2015**, *48*, 530−537.
(71) Moore, B., II; Charaf-Eddin, A.; Planchat, A.; Adamo, C.; Autschbach, J.; Jacquemin, D. Electronic Band Shapes Calculated with Optimally Tuned Range-Separated Hybrid Functionals. *J. Chem. Theory Comput.* **2014**, *10*, 4599−4608.
(72) Jacquemin, D.; Moore, B., II; Planchat, A.; Adamo, C.; Autschbach, J. Performance of an Optimally Tuned Range-Separated Hybrid Functional for 0−0 Electronic Excitation Energies. *J. Chem. Theory Comput.* **2014**, *10*, 1677−1685.
(73) Grimme, S.; Neese, F. Double-Hybrid Density Functional Theory for Excited Electronic States of Molecules. *J. Chem. Phys.* **2007**, *127*, 1541161−1541168.
(74) Filatov, M.; Huix-Rotllant, M. Assessment of Density Functional Theory based Delta SCF (Self-Consistent Field) and Linear Response Methods for Longest Wavelength Excited States of Extended pi-Conjugated Molecular Systems. *J. Chem. Phys.* **2014**, *141*, 0241121−0241129.
(75) Minezawa, N. Vertical Excitation Energies of Linear Cyanine Dyes by Spin-Flip Time-Dependent Density Functional Theory. *Chem. Phys. Lett.* **2015**, *622*, 115−119.
(76) Masunov, A. E. Theoretical Spectroscopy of Carbocyanine Dyes Made Accurate by Frozen Density Correction to Excitation Energies Obtained by TD-DFT. *Int. J. Quantum Chem.* **2010**, *110*, 3095−3100.
(77) Zhekova, H.; Krykunov, M.; Autschbach, J.; Ziegler, T. Applications of Time Dependent and Time Independent Density Functional Theory to the First pi to pi* Transition in Cyanine Dyes. *J. Chem. Theory Comput.* **2014**, *10*, 3299−3307.
(78) Croitor, L.; Coropceanu, E. B.; Masunov, A. E.; Rivera-Jacquez, H. J.; Siminel, A. V.; Fonari, M. S. Mechanism of Nonlinear Optical Enhancement and Supramolecular Isomerism in 1D Polymeric Zn(II) and Cd(II) Sulfates with Pyridine-4-aldoxime Ligands. *J. Phys. Chem. C* **2014**, *118*, 9217−9227.
(79) Mikhailov, I. A.; Musial, M.; Masunov, A. E. Permanent Dipole Moments and Energies of Excited States from Density Functional Theory Compared with Coupled Cluster Predictions: Case of para-Nitroaniline. *Comput. Theor. Chem.* **2013**, *1019*, 23−32.
(80) Yurenev, P. V.; Kretov, M. K.; Scherbinin, A. V.; Stepanov, N. F. Environmental Broadening of the CTTS Bands: The Hexaammineruthenium(II) Complex in Aqueous Solution. *J. Phys. Chem. A* **2010**, *114*, 12804−12812.
(81) Kretov, M. K.; Iskandarova, I. M.; Potapkin, B. V.; Scherbinin, A. V.; Srivastava, A. M.; Stepanov, N. F. Simulation of Structured T-4(1) -> (6)A(1) Emission Bands of Mn2+ Impurity in Zn2SiO4: a First-Principle Methodology. *J. Lumin.* **2012**, *132*, 2143−2150.
(82) Kretov, M. K.; Scherbinin, A. V.; Stepanov, N. F. Simulating the Structureless Emission Bands of Mn2+ Ions in ZnCO3 and CaCO3Matrices by Means of Quantum Chemistry. *Russ. J. Phys. Chem. A* **2013**, *87*, 245−251.
(83) Rukin, P. S.; Freidzon, A. Y.; Scherbinin, A. V.; Sazhnikov, V. A.; Bagaturyants, A. A.; Alfimov, M. V. Vibronic Bandshape of Absorption Spectra of Dibenzoylmethanatoboron Difluoride Derivatives: Analysis Based on Ab Initio Calculations. *Phys. Chem. Chem. Phys.* **2015**, DOI: 10.1039/C5CP02085A.
(84) Heller, E. J. The Semi-Classical Way To Molecular-Spectroscopy. *Acc. Chem. Res.* **1981**, *14*, 368−375.
(85) Lax, M. The Franck-Condon Principle and its Application to Crystals. *J. Chem. Phys.* **1952**, *20*, 1752−1760.
(86) Petrenko, T.; Neese, F. Analysis and Prediction of Absorption Band Shapes, Fluorescence Band Shapes, Resonance Raman Intensities, and Excitation Profiles using the Time-Dependent Theory of Electronic Spectroscopy. *J. Chem. Phys.* **2007**, *127*, 1643191−1643196.
(87) Petrenko, T.; Neese, F. Efficient and Automatic Calculation of Optical Band Shapes and Resonance Raman Spectra for Larger Molecules within the Independent Mode Displaced Harmonic Oscillator Model. *J. Chem. Phys.* **2012**, *137*, 2341071−2341076.
(88) Neese, F.; Petrenko, T.; Ganyushin, D.; Olbrich, G. Advanced Aspects of Ab Initio Theoretical Optical Spectroscopy of Transition

DOI: 10.1021/acs.jpca.5b03877
J. Phys. Chem. A XXXX, XXX, XXX−XXX

Metal Complexes: Multiplets, Spin-Orbit Coupling and Resonance Raman Intensities. *Coord. Chem. Rev.* **2007**, *251*, 288−327.
(89) Tao, J. M.; Perdew, J. P.; Staroverov, V. N.; Scuseria, G. E. Climbing the Density Functional Ladder: Nonempirical Meta-generalized Gradient Approximation Designed for Molecules and Solids. *Phys. Rev. Lett.* **2003**, *91*, 1464011−1464015.
(90) Boese, A. D.; Handy, N. C. New Exchange-Correlation Density Functionals: The Role of the Kinetic-Energy Density. *J. Chem. Phys.* **2002**, *116*, 9559−9569.
(91) Becke, A. D. Density-Functional Thermochemistry. 3. The Role of Exact Exchange. *J. Chem. Phys.* **1993**, *98*, 5648−5652.
(92) Adamo, C.; Barone, V. Toward Reliable Density Functional Methods without Adjustable Parameters: the PBE0Model. *J. Chem. Phys.* **1999**, *110*, 6158−6170.
(93) Mikhailov, I. A.; Bondar, M. V.; Belfield, K. D.; Masunov, A. E. Electronic Properties of a New Two-Photon Absorbing Fluorene Derivative: The Role of Hartree-Fock Exchange in the Density Functional Theory Design of Improved Nonlinear Chromophores. *J. Phys. Chem. C* **2009**, *113*, 20719−20724.
(94) Zhao, Y.; Truhlar, D. G. Density Functional for Spectroscopy: No Long-Range Self-Interaction Error, Good Performance for Rydberg and Charge-Transfer States, and Better Performance on Average than B3LYP for Ground States. *J. Phys. Chem. A* **2006**, *110*, 13126−13130.
(95) Zhao, Y.; Truhlar, D. G. The M06 Suite of Density Functionals for Main Group Thermochemistry, Thermochemical Kinetics, Noncovalent Interactions, Excited States, and Transition Elements: Two New Functionals and Systematic Testing of Four M06-Class Functionals and 12 Other Functionals. *Theor. Chem. Acc.* **2008**, *120*, 215−241.
(96) Boese, A. D.; Martin, J. M. L. Development of Density Functionals for Thermochemical Kinetics. *J. Chem. Phys.* **2004**, *121*, 3405−3416.
(97) Peverati, R.; Zhao, Y.; Truhlar, D. G. Generalized Gradient Approximation That Recovers the Second-Order Density-Gradient Expansion with Optimized Across-the-Board Performance. *J. Phys. Chem. Lett.* **2011**, *2*, 1991−1997.

DOI: 10.1021/acs.jpca.5b03877
J. Phys. Chem. A XXXX, XXX, XXX−XXX